

## Preparation of Polyacrylamide/Graphite Oxide Superabsorbent Nanocomposites with Salt Tolerance and Slow Release Properties

Zhao-Qi Zhu, Han-Xue Sun, Gui-Xian Li, Wei-Dong Liang, Xue-Mei Bao, Jin An, Pei-Qing La, Jian-Feng Dai, An Li

State Key Laboratory of Gansu Advanced Non-ferrous Metal Materials, Key Laboratory of Non-ferrous Metal Alloys and Processing, Ministry of Education, College of Petrochemical Technology, Lanzhou University of Technology, Lanzhou, 730050, People's Republic of China

Correspondence to: J.-F. Dai (E-mail: daijf@lut.cn) or A. Li (E-mail: lian2010@lut.cn)

**ABSTRACT:** Novel polyacrylamide/graphite oxide (PAM/GO) superabsorbent nanocomposites were synthesized by a simple solution polymerization of acrylamide using *N,N'*-methylenebisacrylamide as crosslinker and ammonium persulfate as initiator. The well dispersion of GO nanoplatelets in the polymeric network results in a remarkable improvement on the comprehensive swelling performance of the resulting superabsorbent nanocomposites. The water absorption experimental results show that the superabsorbent nanocomposites could absorb water as twice as that of crosslinked polyacrylamide (PAM) superabsorbent with a weight gain of  $400 \text{ g g}^{-1}$  with a low loading of GO. The salt tolerance and water-retention ability of the resulting PAM/GO superabsorbent nanocomposites are also enhanced compared with PAM. Moreover, by embedding of ammonium salt into PAM/GO network, the PAM/GO superabsorbent nanocomposites also exhibit a slow release behavior of ammonium salt from network when swelling in water, which makes the PAM/GO superabsorbent nanocomposites multifunctional absorbent materials with great potential for agricultural and horticultural applications. © 2013 Wiley Periodicals, Inc. *J. Appl. Polym. Sci.* 000: 000–000, 2013

**KEYWORDS:** composites; gels; hydrophilic polymers

Received 19 September 2012; accepted 22 December 2012; published online

DOI: 10.1002/app.38965

### INTRODUCTION

Superabsorbents are three-dimensionally crosslinked hydrophilic polymers capable of swelling and retaining a large amount of water in the swollen state and the water absorbed is hardly removable even under some pressure. Due to their superior swelling performance to traditional absorbents (such as sponge, cotton, and pulp, etc.), superabsorbents have attracted much attention in the past several decades and found a variety of valuable applications, such as medicine for drug delivery systems,<sup>1,2</sup> tissue engineering,<sup>3</sup> immobilization of protein and cells,<sup>4,5</sup> agriculture, and horticulture,<sup>6</sup> sanitary products,<sup>7</sup> and so on. To date, extensive efforts have been devoted to develop new superabsorbents with improved swelling performance, in which the employment of various hydrophilic vinyl monomers for changing the polyelectrolytic nature of superabsorbents or tuning the crosslinking density of superabsorbent networks are common approaches. In addition to these traditional methods, the incorporation of micro- or nano-sized fillers into crosslinked polymeric networks for fabrication of novel superabsorbent composites has been proved to be a cost-efficient way to improve the comprehensive

swelling performance of the resulting superabsorbents. For instance, Wu et al.<sup>8,9</sup> prepared starch-*g*-acrylamide/clay and poly(acrylic acid)/mica superabsorbent composites. Li et al.<sup>10</sup> successfully developed novel poly(acryl amide)/laponite clay nanocomposite hydrogels for improving cationic dye adsorption behavior. A series of attapulgite-based superabsorbent composites have also been reported by Li et al.<sup>11,12</sup> It can be seen that the water absorbencies of these superabsorbent composites are enhanced and the production cost is greatly reduced by introducing clay micropowder into polymeric networks. In these cases, the improvement on both swelling performance and salt-tolerance performance of the resulting superabsorbent composites have been realized as the following two reasons: (i) the clay particles in the polymeric network act as additional crosslinking points which form a more intact polymeric network structure and then the network has additional space to allow more water to be held; (ii) the non-ionic nature of clay particles in polymeric network can efficiently resist against the collapse of the polyelectrolytic network in saline solutions. Inspired by this, more recently we have successfully developed novel

superabsorbent nanocomposites by introduction of graphite oxide (GO) nanoplatelets into crosslinked poly(acrylic acid) network and the expected enhancement on both water absorbency and salt-tolerance has been achieved.<sup>13</sup>

Recently, studies on superabsorbents with the slow-release property of fertilizer have received considerable attention. In comparison with normal superabsorbents, these superabsorbents have great advantages due to not only their swelling performance but also their slow-release properties.<sup>14,15</sup> In addition, these superabsorbents with the slow-release property of fertilizer can be used as functional water-management materials and may prove especially practical in agricultural and horticultural applications. In a continuation of our studies on absorbent materials,<sup>13,16,17</sup> in this work we report the design and preparation of novel GO-based superabsorbent nanocomposites with the slow-release property of fertilizer. The polyacrylamide/GO (PAM/GO) superabsorbent nanocomposites were prepared by incorporation of GO nanoplatelets into PAM matrix by a solution polymerization method using *N,N'*-methylenebisacrylamide as crosslinker and ammonium persulfate as initiator referred to previous work.<sup>13</sup> Our primary design is using non-ionic acrylamide monomer and non-ionic GO nanoplatelets as fillers to improve the swelling performance and salt-tolerance of the resulting superabsorbent nanocomposites, more importantly, the barrier effect of GO nanoplatelets incorporating in polymeric network would possibly offer the network new functionality for slow release of the imbedded fertilizer, which may provide a new possibility for preparation of multifunctional superabsorbent materials and should be of special interest especially in agricultural and horticultural applications.

## EXPERIMENTAL

### Materials

The natural graphite powder used in this study is supplied by Bay Carbon, *N,N'*-methylenebisacrylamide and ammonium persulfate are supplied by Sigma-Aldrich, and other reagents are from Guangdong Guanghua Sci-Tech Co. All reagents do not undergo further purification.

### Experimental Procedure

**Preparation of GO and Composites.** GO was synthesized from graphite powder using a modified Hummers method as follows.<sup>13,18,19</sup> In order to be fully oxidized, the graphite powder is pretreated by  $K_2S_2O_8$ ,  $P_2O_5$ , and  $H_2SO_4$  (98 wt%).<sup>19,20</sup> Then followed the Hummers method, concentration  $H_2SO_4$  (38 mL) and preoxidized graphite (1.0 g) were mixed in an ice bath. Then  $KMnO_4$  (6.0 g) was added into the mixture with the temperature not more than 10°C. The temperature was raised to 35°C for 2 h. Deionized water (77 mL) was added slowly and the suspension was heated to 98°C for 15 min. The suspension was diluted with deionized water (100 mL) and 30%  $H_2O_2$  (5.0 mL), then washed fully with aqueous HCl (3 wt%) solution and water. The wet gel was dried at 50°C for 3 days and milled to GO powder. For preparation of polyacrylamide(PAM)-GO superabsorbent nanocomposite, 20 mL colloidal suspension of GO (the concentration is 0.05 wt%) and 7.1 g acrylamide are mixed and sonicated until the mixture became clear. The obtained brown dispersion is subjected to 10 min of centrifugation at 4000 rpm for removal of bigger suspended particles. At

the room temperature and under an inert atmosphere, 7.1 mg *N,N'*-methylenebisacrylamide is added with vigorously stirring. After 15 min, the temperature is raised to 30–35°C and 80 mg ammonium persulfate is quickly added. As the temperature slowly increases, the mixture becomes brown jelly at 50–55°C along with bubbles, after which the colloid substance is maintained at 70°C for 3 h. Then in the air atmosphere, the resulting composite PAM/GO1 (the composite of GO with the starting concentration of 0.1 wt% is defined PAM/GO2) is washed with abundant water and dried at 60°C to a constant weight, and then milled and screened with a particle size in the range of 60–80 mesh. PAM is prepared similarly to the composite without GO dispersion.

**Water-absorbency Measurement.** Before measurement, the samples were dried overnight in vacuum at 60°C. The absorbency value was gained by immersing the composite (0.1 g) in distilled water, water with various pH values which was adjusted by adding HCl or NaOH into water, aqueous NaCl (0.5 wt%), and  $MgCl_2$  (0.5 wt%) at room temperature. After reaching the swelling–deswelling equilibrium, swollen sample was separated from the solution by filtering over 80-mesh screen. The water-absorbency  $M_{H_2O}$  ( $g\ g^{-1}$ ) was calculated by the equation as follows:

$$M_{H_2O} = (m_2 - m_1) / m_1$$

where  $m_1$  and  $m_2$  are the weights of the dry sample and the water-swollen sample.

### Characterization

The elemental contents were obtained from Elementar Vario EL and X-ray powder diffraction (XRD) measurements were performed on a Rigaku D/Max-2400 with a Cu tube source. Solid state infrared spectra (IR) were recorded from in the range of 4000–400  $cm^{-1}$  using the KBr pellet technique on a FT-Raman Module (Nicolet, America) instrument. Thermogravimetric analysis (TGA) was performed under a nitrogen flow rate of 20  $mL\ min^{-1}$  using a Perkin-Elmer TG/DTA-6300 instrument and the sample was heated from room temperature to 600°C at 10°C  $min^{-1}$ . The morphology of dried samples was examined by scanning electron microscopy (SEM, JSM-6701F) after coating the samples with Au film. Atomic force microscopy (AFM) image of GO was obtained using Scanning Probe Microscope (SPM) from AIST-NT Inc.

## RESULTS AND DISCUSSION

The GO nanoplatelets were prepared by the oxidation of pristine graphite by a modified Hummer's method. During the oxidation treatment of pristine graphite, the graphene sheets in graphite are heavily oxygenated and the resulting GO nanoplatelets can be exfoliated to form stable aqueous dispersion by ultrasonic treatment. The AFM image of GO nanoplatelet is shown in Figure 1. The GO nanoplatelet exhibits a thickness of approximately 2 nm, which indicates that the GO nanoplatelets are in multilayer structures. Further measurement results show that the thickness of the most GO nanoplatelets samples ranges from 1 to 2 nm under our experimental conditions. The XRD patterns for graphite, GO, PAM, and PAM/GO2 superabsorbent nanocomposite are shown in Figure 2(a). It is clear that the

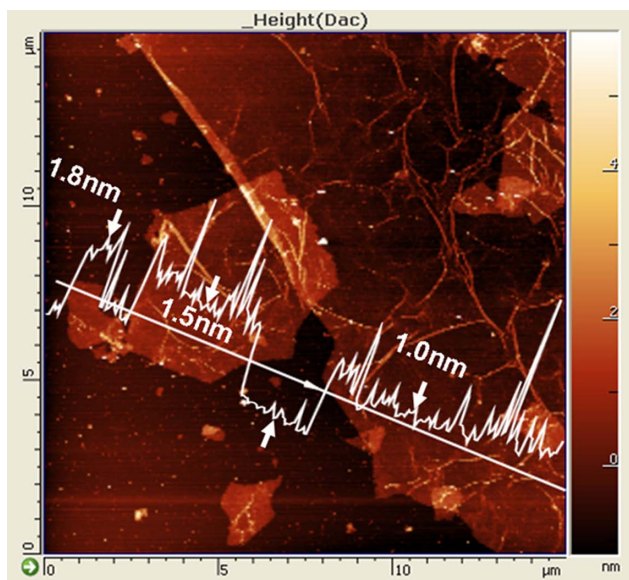


**Figure 1.** A typical AFM non-contact-mode image of a GO nanoplatelet deposited onto a freshly cleaved mica from an aqueous dispersion. [Color figure can be viewed in the online issue, which is available at [wileyonlinelibrary.com](http://www.wileyonlinelibrary.com).]

peak for GO phase appeared at  $12.2^\circ$ , in contrast, the characteristic peak of graphite at  $26.6^\circ$  disappeared, indicating that the successful synthesis of GO by oxidation of graphite. These

results are in good agreement with previous literatures.<sup>13,21</sup> The distance of interlayer of GO were calculated to be  $7.30\text{\AA}$  larger than that of  $3.34\text{\AA}$  for natural graphite, indicating the increasing of interlayer distance due to the oxidation. The chemical composition of initial graphite was measured to be C: 77.43%, H: 1.29%, and O: 21.28%, after oxidation, the chemical composition of as-prepared GO samples was changed to be C: 45.18%, H: 2.48%, and O: 52.34% by elemental analysis, showing the increasing of oxygen content. Moreover the XRD pattern of PAM/GO2 superabsorbent nanocomposite reveals that there are no obvious changes in diffraction profile compared to that of PAM, implying that the PAM/GO2 has the same amorphous feature as that of crosslinked PAM. On the other hand, the peak at  $12.2^\circ$  for GO phase disappeared, suggesting the occurrence of the exfoliation and the decrease of agglomeration of GO nanoplatelets in polymeric matrix.<sup>13</sup> The same observation was also found in polymer intercalated GO as reported previously.<sup>22</sup> As a result, the dispersion of GO nanoplatelets individually in polymeric matrix may be achieved under our experimental conditions, which would expect to improve the comprehensive performance of the resulting products.

The SEM images of GO powders, dried PAM and PAM/GO2 samples are shown in Figure 2(b–d). As shown in Figure 2(b), the GO nanoplatelets with layered structures are irregularly aggregated together to some extent after oxidation. The PAM sample shows a smooth and neat surface morphology [Figure 2(c)], while the surface morphology of PAM/GO2 sample turns

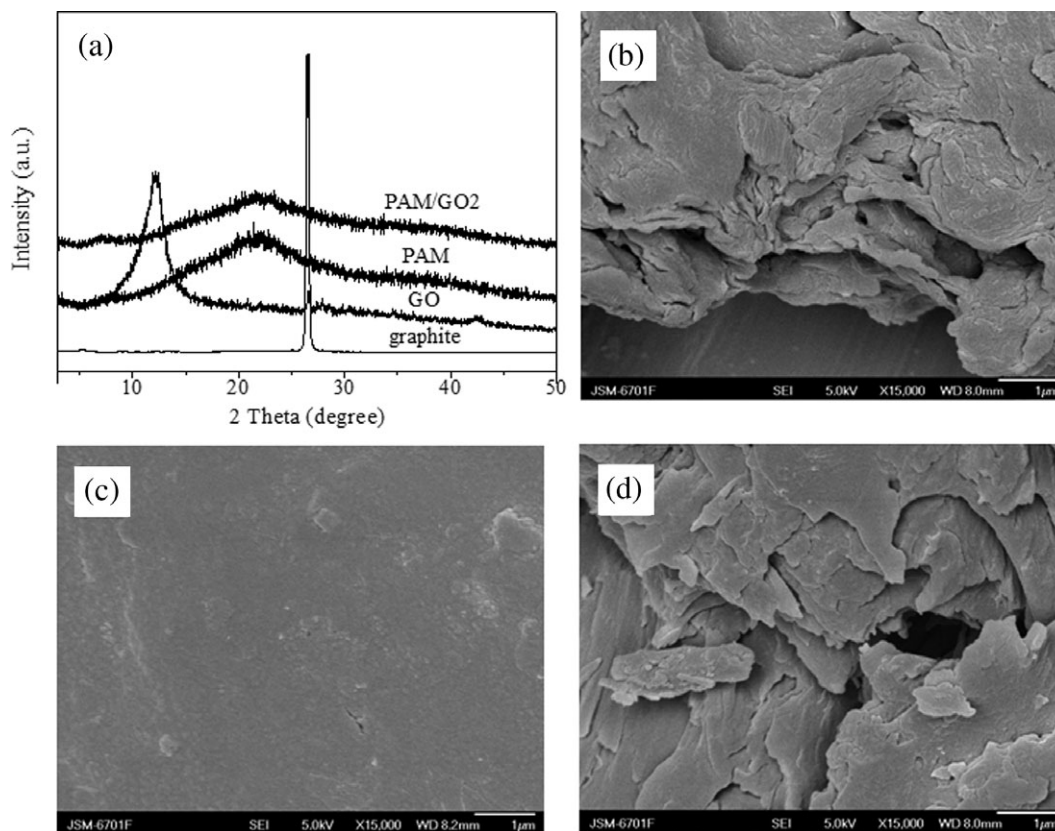


**Figure 2.** (a) XRD patterns of graphite, GO, PAM, and PAM/GO2, and SEM images of (b) GO, (c) PAM and (d) PAM/GO2. Scale bar:  $1\ \mu\text{m}$ .

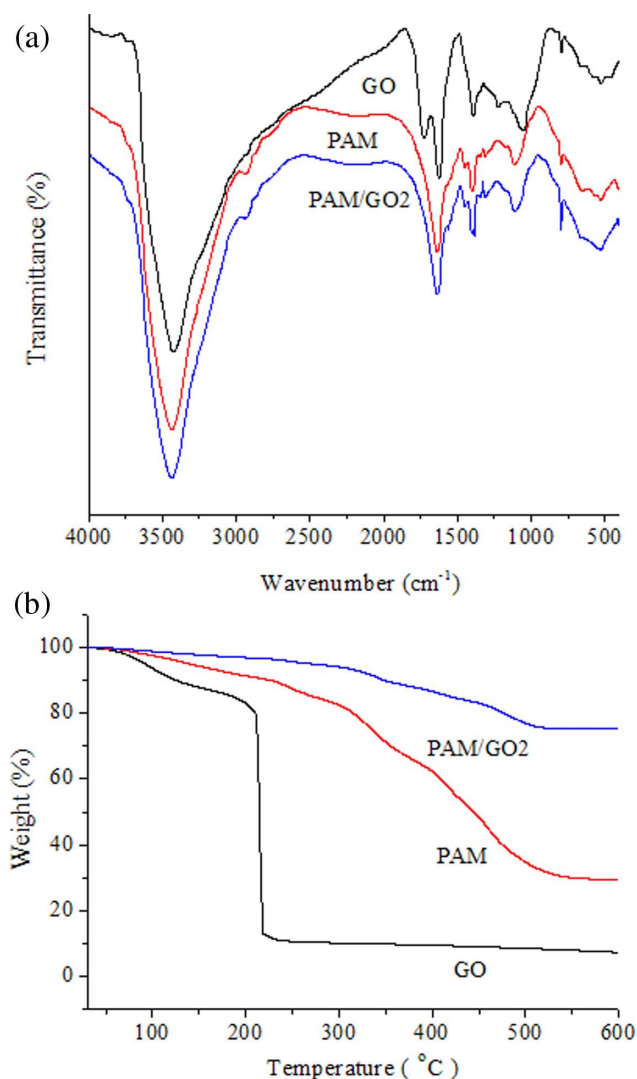


**Figure 3.** (a) IR spectra and (b) TGA curves of GO, PAM, and PAM/GO2. [Color figure can be viewed in the online issue, which is available at [wileyonlinelibrary.com](http://wileyonlinelibrary.com).]

to be more crumpled and rough and with an irregular, plat-like structure after introduction of GO nanoplatelets into PAM network [Figure 2(d)], which may be induced by the layered structure of GO nanoplatelets. IR spectra of GO, PAM, and PAM/GO2 are shown in Figure 3(a). For GO, the intense and broad bands at  $3410\text{ cm}^{-1}$  is attributed to the hydroxyl groups and water molecules. The peak at  $1720\text{ cm}^{-1}$  can be ascribed to the stretching vibration of carboxyl groups on the edges of the layer plane, the peak at  $1630\text{ cm}^{-1}$  is ascribed to the vibration of water molecules, while the peak at  $1390\text{ cm}^{-1}$  and  $1050\text{ cm}^{-1}$  are assigned to the vibrations of O—H and C—O bonds. IR analysis for GO prepared under our experimental conditions is in good agreement with that reported previously.<sup>23</sup> We can therefore infer that GO is rich of oxygen-containing functional groups which would be responsible for the hydrophilic nature of GO. Owing to its hydrophilic nature, the dispersion of GO in water can be easily obtained by ultrasonic treatment and available to react with acrylamide by aqueous polymerization

method for preparing superabsorbent nanocomposites as expected. For PAM, the peaks observed at  $3430\text{ cm}^{-1}$  should be attributed to N—H stretching and water peak. The peak at  $2940\text{ cm}^{-1}$  is corresponding to the C—H stretching of acrylamide units. And the peak at  $1640\text{ cm}^{-1}$  and  $1390\text{ cm}^{-1}$  is attributed to C=O and C—N of amide units. The appearance of these characteristic peaks of both GO and PAM in the IR spectrum of PAM/GO2 composite indicates that GO was successfully incorporated into the polymeric matrix.

The thermal properties for GO, PAM, and PAM/GO2 superabsorbent nanocomposites were investigated by TGA. As shown in Figure 3(b), GO, PAM, and the PAM/GO2 have a very low mass loss below  $100^\circ\text{C}$  implying a loss of moisture. The major weight loss of GO starts at around  $210^\circ\text{C}$  due to the decomposition of oxygen-containing groups, whereas the PAM and PAM/GO2 have a major weight loss starting at around  $300^\circ\text{C}$  and  $350^\circ\text{C}$ . Under the measurement condition, the whole weight loss of GO, PAM, and PAM/GO2 were found to be 92.76 wt%, 70.75 wt%, and 24.93 wt%. Obviously, the thermal stability of nanocomposite is enhanced largely by the introduction of GO into the polymeric network, which is very similar to the enhancement of heat resistance when introduction of clay into the PAM polymeric network. In this case, the “heat barriers” was attributed to the layered structure of clay which could slow down the heat transmission and the volatilization of decomposed products thus in turn enhancing the thermal stability. The enhancement of thermal stability of PAM/GO2 could be explained in the same way.

The swelling performance of PAM, PAM/GO1 and PAM/GO2 were investigated by immersing samples into distilled water, saline solutions, and water with various pH values to reach their swelling equilibrium followed by separation and weighing of the swollen samples. As shown in Figure 4(a), PAM exhibits an absorbency of  $200.46\text{ g g}^{-1}$  in distilled water. The swelling ability of a hydrogel mainly depended on the hydrophilicity of the polymer chains and the physical structure of the polymer. In this case, lots of hydrophilic amine groups bonded in polymer chain, and the spacious network was formed in the polymerization of acrylamide which supplied residences for water molecules. For GO incorporated samples, the water absorbency was found to be  $332.69\text{ g g}^{-1}$  for PAM/GO1 and  $400.11\text{ g g}^{-1}$  for PAM/GO2. Obviously, the introduction of GO into the PAM matrix leads to an enhancement of water absorbency of the resulting samples which may be due to the fact that the hydrophilic groups such as —COOH in edges of the GO layer plane react with —NH<sub>2</sub> of polymers network and produce more stable and intact network for accommodating more water molecules.<sup>8,13</sup> Similar results were also found for mica or attapulgite-based superabsorbent composites.<sup>9,12</sup> However, in most cases, obvious improvement of clay-based superabsorbent composite was only achieved with an inorganic filler loading higher than 5 wt%. In this case, only a very small loading of GO in superabsorbent nanocomposites can lead to a significant enhancement on its swelling performance, which may prove to be an efficient way for development of novel and high performance nanocomposites by using GO nanoplatelets as nano-sized fillers.

We also investigated the swelling performance of PAM, PAM/GO1, and PAM/GO2 in water with various pH values. As

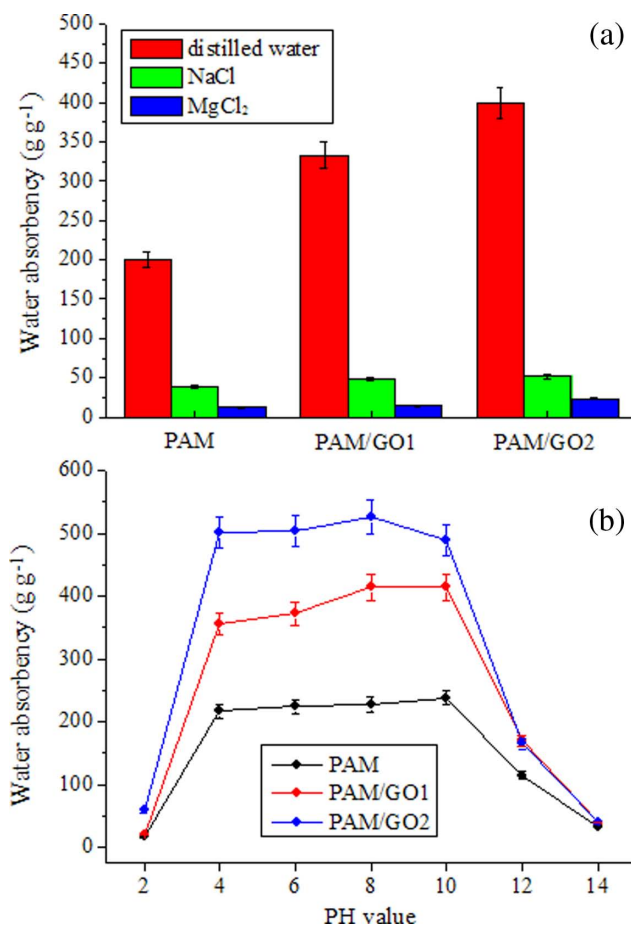


**Figure 4.** (a) Weight gain of PAM, PAM/GO1, and PAM/GO2 in distilled water and salt solutions. (b) Weight gain of PAM, PAM/GO1, and PAM/GO2 in solution of different pH value. [Color figure can be viewed in the online issue, which is available at [wileyonlinelibrary.com](http://wileyonlinelibrary.com).]

shown in Figure 4(b), the change of the water absorbencies for all of three samples is slight in the range of pH value from 4 to 10 and the absorbency is approximately equal to its equilibrium water absorbency for each sample. However, the samples show a sharp decrease in water absorbency in water with both high and low pH value, which are attributed to the decrease of osmotic pressure difference between the polymeric network and the external solution as the ionic strength of external solution increases significantly both in high and low pH value.<sup>11,24</sup>

The swelling performance of PAM, PAM/GO1, and PAM/GO2 in various saline solutions was also investigated. As shown in Figure 4(a), compared with that of in distilled water, the absorbencies for all three samples decrease evidently in NaCl solutions. The absorbency was evaluated to be 37.75 g g<sup>-1</sup>, 48.17 g g<sup>-1</sup>, and 51.59 g g<sup>-1</sup> for PAM, PAM/GO1, and PAM/GO2. In divalent cation solution, in this case is MgCl<sub>2</sub>, the decrease in water absorbencies for three samples are more apparent. The decrease of absorbency in saline solutions should be attributed to the decrease of osmotic pressure difference between the polymeric network and the external solution and complex flocculation ability of PAM to metal ions which induced the formation of intramolecular and intermolecular complexes, which resulted

in the collapse of the polymeric network.<sup>12,25</sup> However, compared to that of PAM, the GO-based samples show a better water absorbency in both NaCl and MgCl<sub>2</sub> solutions, indicating an improved salt tolerance effect by introduction of GO into PAM network. Compared to those ionic vinyl monomers such as acrylic acid, acrylamide is a kind of nonionic monomer and has great advantage on its good salt-tolerance performance as a raw material for superabsorbent.<sup>26</sup> So, the good water absorbency both in distilled water and saline solutions for PAM/GO1 and PAM/GO2 should be attributed to the fact that the GO sheets in polymeric network act as “nonionic” nanofillers to effectively improve the network structures and enhance the swelling performance in saline solutions. Compared with poly(-acrylic acid)/GO superabsorbent composites,<sup>13</sup> PAM/GO shows a better absorbency in saline water due to the intrinsic non-polyelectrolytic network of PAM.

The water retention of the swollen absorbent composites was investigated by a heating test at 100°C and centrifugation at 4000 rpm. As shown in Figure 5(a). It can be seen that a decreasing trend was observed for all of three samples with prolonging the test time. Keeping at 100°C for 50 min, the water

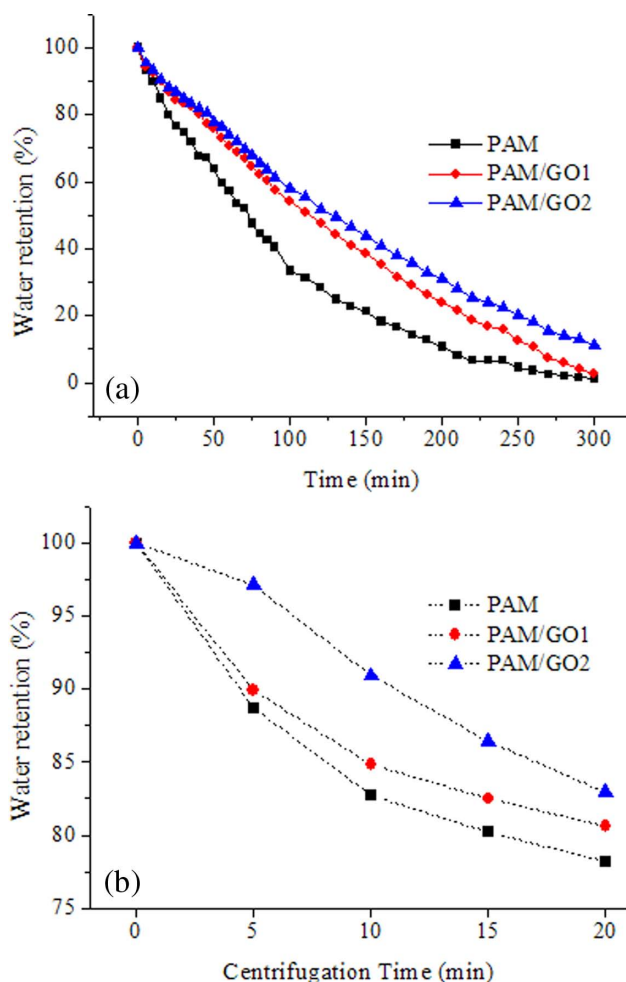


**Figure 5.** Water retention of swollen samples as a function of time at 100°C (a) and with centrifugation at 4000 rpm (b). [Color figure can be viewed in the online issue, which is available at [wileyonlinelibrary.com](http://wileyonlinelibrary.com).]

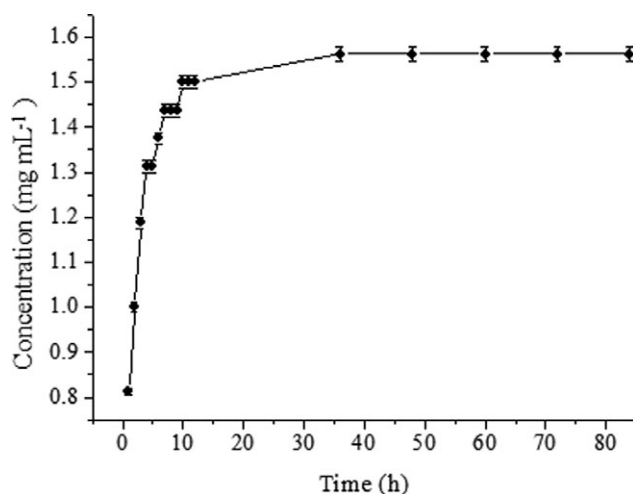


Figure 6. The release curve of  $(\text{NH}_4)_2\text{SO}_4$  in PGAS.

retention was 63.67%, 74.85%, and 77.98% for PAM, PAM/GO1, and PAM/GO2. Clearly, GO-based samples have better water retention than PAM in the test conditions. The similar results were also obtained in the centrifugation test [Figure 5(b)]. After centrifugation for 20 min, 82.9% of water maintained in PAM/GO2, while 78.2% and 80.6% of water maintained in PAM and PAM/GO1, respectively. According to previous literatures,<sup>27</sup> three forms of water could exist in hydrogel, including bond-water, half bond-water, and free water. The free water is more mobile and easily lost than bond-water and half bond-water. As mentioned in our previous study,<sup>13</sup> the irregular dispersion of the plate-like GO nanoplatelets in polymeric network may form so-called “house-of-cards” structures which could serve as barriers to hinder the diffusion of free water in network, which would be also responsible for the slower release of water from PAM/GO nanocomposites than that of from PAM in this case.

Inspired by this observation, it would be naturally assumed that the PAM/GO superabsorbent nanocomposites should be ideal candidates as carriers for slow release of fertilizer. As a proof-of-concept study, therefore, we also investigated the slow release property of PAM/GO by embedding of  $(\text{NH}_4)_2\text{SO}_4$  into the network of nanocomposites. The slow release experiment was performed as follows. The wet gel (15.0 g) containing  $(\text{NH}_4)_2\text{SO}_4$  (0.75 g) (named as PGAS) was immersed into 300 mL distilled water. At certain time intervals, 10 mL of the solution containing  $(\text{NH}_4)_2\text{SO}_4$  was sampled for testing with the formaldehyde method. Then an additional 10 mL of distilled water was added into the beaker in order to maintain a constant amount of the solution. The release trend of  $(\text{NH}_4)_2\text{SO}_4$  is shown in Figure 6 and around 95.8% of  $(\text{NH}_4)_2\text{SO}_4$  was released in the whole test time. According to Raban and Shaviv description,<sup>28</sup> the release process of polymer-coated fertilizer can be divided into three periods: (i) the initial stage during which water molecules diffusing into the network made the hydrogel swelling, and almost no obvious releasing is observed. (ii) The constant releasing stage during which  $(\text{NH}_4)_2\text{SO}_4$  release from the network of hydrogel driven by the concentration difference between hydrogel and solution accompanied with polymer swollen in water.

(iii) Gradual decay of release rate stage. In this period, the release became slow with the decrease of driving force for the release. It can be seen from Figure 6 that the release behavior of PGAS is slightly different from that of the polymer-coated fertilizer such as urea as reported previously.<sup>29</sup> Unlike urea, due to the ionic nature of  $(\text{NH}_4)_2\text{SO}_4$ , the doped  $(\text{NH}_4)_2\text{SO}_4$  quickly released from network driven by osmotic pressure difference between the polymeric network and the external solution when the sample was immersed in water at the initial stage. So the initial release rate for  $(\text{NH}_4)_2\text{SO}_4$  is higher than that of urea. However, for the whole duration time, the release rate for PGAS is lower than that of polymer-coated urea and about 95.8% of the doped  $(\text{NH}_4)_2\text{SO}_4$  can be released after 36 h, which makes the PAM/GO an ideal candidate as an efficient fertilizer carrier with great potential for agricultural and horticultural applications. Similar to that of slow release of water molecules from PAM/GO samples, the barrier effect of plate-like GO nanoplatelets in network would also be responsible to the slow release behavior of  $(\text{NH}_4)_2\text{SO}_4$  for PGAS. Inspired by these results, further tailoring the properties of GO-based superabsorbent nanocomposites with controlled release behavior for fertilizer can be anticipated and the work in this direction is currently underway.

## CONCLUSIONS

GO nanoplatelets as layered fillers were introduced into the PAM matrix to prepare superabsorbent composites by solution polymerization. Our results exhibited the superabsorbent nanocomposites show water absorbency of  $332.69 \text{ g g}^{-1}$  and  $400.11 \text{ g g}^{-1}$  for PAM/GO1 and PAM/GO2 with low loading of 0.037 wt% and 0.074 wt% of GO. The salt tolerance and water-retention ability of the resulting PAM/GO superabsorbent nanocomposites are also enhanced. Moreover, the as-synthesized superabsorbent nanocomposites exhibit slow release behavior of  $(\text{NH}_4)_2\text{SO}_4$ , which makes them multifunctional materials for both water management and slow release of fertilizer and may have great potential especially for agricultural and horticultural applications.

## ACKNOWLEDGMENTS

The authors are grateful to the National Natural Science Foundation of China (Grant No. 51263012, 51262019, 51164022), the Natural Science Foundation of Gansu Province, China (Grant No. 1112RJZA020), Open Fund of State Key Laboratory, Lanzhou University of Technology (Grant No. SKL12011) and the starting-funding of Lanzhou University of Technology.

## REFERENCES

1. Qiu, Y.; Park, K. *Adv. Drug Delivery Rev.* **2001**, *53*, 321.
2. Hoare, T. R.; Kohane, D. S. *Polymer* **2008**, *49*, 1993.
3. Lee, K. Y.; Mooney, D. J. *Chem. Rev.* **2001**, *101*, 1869.
4. Patel, M. P.; Pavlovic, P.; Hughes, F. J.; King, G. N.; Cruchley, A.; Braden, M. *Biomaterials* **2001**, *22*, 2081.
5. Horak, D.; Kroupova, J.; Slouf, M.; Dvorak, P. *Biomaterials* **2004**, *25*, 5249.

6. Tohidi-Moghadam, H. R.; Shirani-Rad, A. H.; Nour-Mohammadi, G.; Habibi, D.; Mashhadi-Akbar-Boojar, M. *Am. J. Agric. Biol. Sci.* **2009**, *4*, 215.
7. Garner, C. M.; Nething, M.; Nguyen, P. *J. Chem. Ed.* **1997**, *74*, 95.
8. Wu, J. H.; Lin, J. M.; Zhou, M.; Wei, C. R. *Macromol. Rapid Commun.* **2000**, *21*, 1032.
9. Lin, J. M.; Wu, J. H.; Yang, Z. F.; Pu, M. L. *Rapid Commun.* **2001**, *22*, 422.
10. Li, P.; Siddaramaiah; Kim, N. H.; Heo, S. B.; Lee, J. H. *Compos. Part B* **2008**, *39*, 756.
11. Li, A.; Wang, A. Q.; Chen, J. M. *J. Appl. Polym. Sci.* **2004**, *92*, 1596.
12. Li, A.; Zhang, J.; Wang, A. Q. *J. Appl. Polym. Sci.* **2007**, *103*, 37.
13. Zhu, Z. Q.; Sun, H. X.; Qin, X. J.; Wang, L.; Pei, C. J.; Wang, L.; Zeng, Y. Q.; Wen, S. H.; La, P. Q.; Li, A. *J. Mater. Chem.* **2012**, *22*, 4811.
14. Zhan, F. L.; Liu, M. Z.; Guo, M. Y.; Wu, L. *J. Appl. Polym. Sci.* **2004**, *92*, 3417.
15. Li, A.; Zhang, J.; Wang, A. Q. *Bioresour Technol.* **2007**, *98*, 327.
16. Li, A.; Sun, H. X.; Tan, D. Z.; Fan, W. J.; Wen, S. H.; Qing, X. J.; Li, G. X.; Li, S. Y.; Deng, W. Q. *Energy Environ. Sci.* **2011**, *4*, 2062.
17. Wang, Y.; Li, A.; Wang, K.; Guan, C.; Deng, W. Q.; Li, C.; Wang, X. *J. Mater. Chem.* **2010**, *20*, 6490.
18. Hummers, W. S.; Offeman, R. E. *J. Am. Chem. Soc.* **1958**, *80*, 1339.
19. Kovtyukhova, N. I.; Ollivier, P. J.; Martin, B. R.; Mallouk, T. E.; Chizhik, S. A.; Buzaneva, E. V.; Gorchinskiy, A. D. *Chem. Mater.* **1999**, *11*, 771.
20. Gilje, S.; Han, S.; Wang, M.; Wang, K.; Kaner, R. *Nano Lett.* **2007**, *7*, 3394.
21. Jeong, H. K.; Jin, M. H.; So, K. P.; Lim, S. C.; Lee, Y. H. *J. Phys. D Appl. Phys.* **2009**, *42*, 065418.
22. Wu, J.; Tang, Q.; Sun, H.; Lin, J.; Ao, H.; Huang, M.; Huang, Y. *Langmuir* **2008**, *24*, 4800.
23. Jeong, H. K.; Lee, Y. P.; Lahaye, R. J.; Park, M. H.; An, K. H.; Kim, I. J.; Yang, C. W.; Park, C. Y.; Ruoff, R. S.; Lee, Y. H. *J. Am. Chem. Soc.* **2008**, *130*, 1362.
24. Huang, Y.; Zeng, M.; Ren, J.; Wang, J.; Fan, L.; Xu, Q. *Colloids Surf. A* **2012**, *401*, 97.
25. Arinaitwe, E.; Pawlik, M. *Int. J. Miner. Process.* **2009**, *91*, 50.
26. Li, A.; Wang, A. Q. *Eur. Polym. J.* **2005**, *41*, 1630.
27. Lee, W. F.; Wu, R. J. *J. Appl. Polym. Sci.* **1997**, *64*, 1701.
28. Shaviv, A.; Raban, S.; Zaidel, E. *Environ. Sci. Technol.* **2003**, *37*, 2257.
29. Liang, R.; Liu, M. *J. Agric. Food Chem.* **2006**, *54*, 1392.